JOURNAL OF MATERIALS SCIENCE 12 (1977) 2200–2208

Impression creep; a new creep test

S. N. G. CHU, J. C. M. LI
Materials Science Program, Department of Mechanical and Aerospace Sciences, University of Rochester, Rochester, New York, USA

A new indentation creep test is introduced in which the indenter is a circular cylinder with a flat end. Unlike conventional indentation tests, a steady-state velocity is observed in this new test shortly after a transient period during which the indenter makes a shallow impression on the surface of the specimen; hence the name "impression creep". This steady-state velocity is found to have the same stress and temperature dependences as the conventional undirectional creep tests using bulk specimens. Three possible mechanisms are analysed in detail, bulk diffusion, surface diffusion, and dislocation creep. They have different stress and indenter-size (radius) dependences. Experimental results on succinonitrile crystals are reported.

1. Introduction

Since conventional creep testing requires many specimens to establish stress and temperature effects, indentation hot hardness is sometimes used as a substitute. Various ways have been proposed to relate creep rate to the time-dependent hardness, but none seems to work very well (for some reviews, see Westbrook [1] and Merchant *et al.* [2]). The reason is very simple: when the hardness decreases with time, the stress decreases also, and no steady state can be achieved.

To avoid such difficulty, the shape of the indenter is changed from a sphere or a pyramid to a circular cylinder of flat end. The punching or indenting stress is thus constant at constant load. Two steady state velocities were found (to be discussed later) for the indenter, one near the surface and the other deep into the specimen. To distinguish these two velocities, the former is called "impression creep" [3] and the latter "penetration creep" [4]. Since the latter may involve friction between the penetrating rod and the specimen, only the former is studied in detail in this paper.

2. Theoretical considerations

Three mechanisms are possible in the indentation creep of single crystals; bulk diffusion, surface diffusion, and dislocation motion. With the circular cylindrical indenter which is much harder than the material, the analyses of these mechanisms are greatly simplified. The diffusion problems are presented here, and the dislocation creep problem will be analysed numerically using finite element method in the next paper. All these results are taken into consideration in the analysis of impression creep measurements.

2.1. Bulk diffusion

The path of vacancy diffusion, shown in Fig. 1, starts from the free surface, passes through the bulk and terminates underneath the punch (cylindrical indenter). The free surface is assumed to be

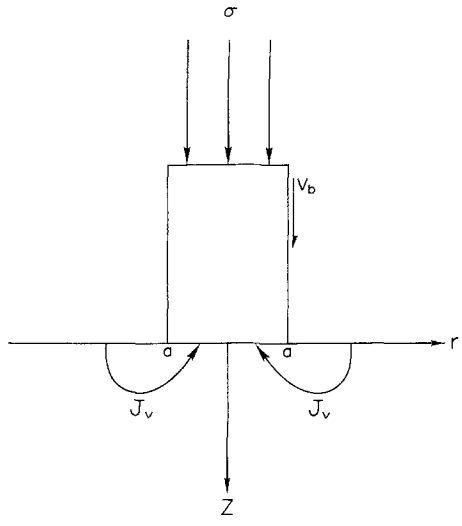

Figure 1 Paths for bulk diffusion.

an efficient source of vacancies so that the vacancy concentration near the surface is maintained at C_v^∞ (moles per unit volume) which is the same as that at large distances from the punch (indenter). The vacancy arrival underneath the punch should be at a rate consistent with the punch (or impressing) velocity v_b:

$$\frac{\partial c_v}{\partial z} = \frac{v_b}{VD_v} \quad \text{at} \quad z = 0, r \leqslant a, \tag{1}$$

where c_v is the concentration (moles per unit volume) of vacancies, V is the molar or atomic volume of atoms, and D_v is the diffusivity of vacancies. For simplicity and within the range of impression creep, Equation 1 is assumed valid at $z = 0$, even though the punch may have impressed somewhat into the surface. When diffusion reaches a steady state, the following Laplace equation is satisfied everywhere inside the crystal:

$$\frac{\partial^2 c_v}{\partial r^2} + \frac{1}{r}\frac{\partial c_v}{\partial r} + \frac{\partial^2 c_v}{\partial z^2} = 0. \tag{2}$$

Equation 2 is solved to satisfy the boundary conditions at $z = 0$; namely Equation 1 for $r \leqslant a$ and constant concentration for $r \geqslant a$. The solution is found to be

$$c_v(r, z) = c_v^\infty - \sqrt{\left(\frac{2}{\pi a}\right)}\frac{a^2 v_b}{VD_v}\int_0^\infty k^{-1/2} e^{-kz} J_0(kr) J_{3/2}(ka)\mathrm{d}k, \tag{3}$$

where the Js are Bessel functions of the first kind.

For $z = 0$, Equation 3 reduces to

$$c_v(r, 0) = c_v^\infty - 2v_b\sqrt{(a^2 - r^2)}/\pi VD_v \quad \text{for} \quad r \leqslant a \tag{4}$$

directly underneath the punch. This concentration distribution, which is needed for steady-state vacancy flow starting from the free surface and ending underneath the punch so as to allow the punch to descend at a velocity v_b, must be maintained mechanochemically by the punching stress. In other words, the driving force for diffusion is supplied by the mechanical work done by the punch:

$$RT\int_0^a \ln(c_v^\infty/c_v)2\pi r\mathrm{d}r = \pi a^2 \sigma V, \tag{5}$$

where R is the gas constant, and T the absolute temperature.

At the limit of small stress, a linear relation is found between the impressing velocity v_b and the punching stress σ;

$$v_b = \frac{3\pi\sigma VD}{4aRT} \tag{6}$$

where $D = D_v c_v^\infty V$ is the self diffusivity of atoms. Equation 6 shows that for the same punching stress, the impressing velocity is inversely proportional to the radius of the punch. Such relation is characteristic for bulk diffusion.

2.2. Surface diffusion

In addition to the bulk diffusion mechanism, the punch can descend due to surface diffusion of atoms or molecules along the interface between the punch and the crystal as shown in Fig. 2. The steady state diffusion problem is simple and the concentration of surface vacancies (moles per unit area), c_{vs}, at r is:

$$c_{vs}^\infty - c_{vs} = \frac{v_s}{4VD_{vs}}(a^2 - r^2) \tag{7}$$

where v_s is the impressing velocity contributed by surface diffusion, c_{vs}^∞ is the surface concentration of vacancies outside the punch which is assumed constant, and D_{vs} is the surface diffusivity of vacancies ($cm^2\ sec^{-1}$). The driving force for diffusion is again supplied by mechanical work done by the punch:

$$RT\int_0^a \ln(c_{vs}^\infty/c_{vs})2\pi r\mathrm{d}r = \pi a^2 \sigma V. \tag{8}$$

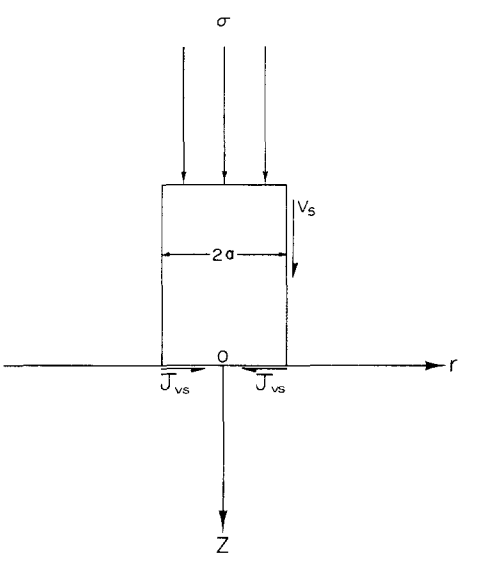

Figure 2 Paths for surface diffusion.

At the limit of small stress, a linear relation between the impressing velocity v_s due to surface diffusion and the punching stress σ is obtained:

$$v_s = \frac{8D_s c_s^\infty V^2 \sigma}{a^2 RT}, \tag{9}$$

where D_s is self surface diffusivity, and c_s^∞ is surface concentration (moles per unit area) of atoms outside the punch. Equation 9 shows that for the same punching stress, the impressing velocity is inversely proportional to the area of the punch, a characteristic for surface diffusion control. In addition to the stress and punch-size dependencies of impressing velocity, the temperature dependence should reveal the activation energy for surface diffusion, which should be smaller than bulk diffusion.

To see the relative magnitudes of v_b and v_s, Equations 7 and 9 can be compared to give

$$\frac{v_b}{v_s} = \frac{3\pi a}{32 c_s^\infty V} \frac{D}{D_s}. \tag{10}$$

For succinonitrile at 45° C, $a = 0.5$ mm, and $D_s/D = 10^4$, this ratio is about 46, indicating that the surface diffusion may not be important unless the punch size is much smaller than 0.5 mm or D_s/D is much larger than 10^4.

2.3. Dislocation creep

Another mechanism of impression creep is by the generation and motion of dislocations. The impressing velocity v_d is calculated numerically by the finite element method and is presented in the next paper. Briefly, a power law constitutive equation is assumed to be valid for each finite element at the steady state. This power law is between the creep rate and the Von Mises stress. Then the Von Mises flow rule is used to calculate the various strain components. Any incompatibility is removed by the development of internal stresses. The calculation is done for many time intervals until a trend toward a steady state is clearly indicated.

The results are as follows: the Von Mises stress available for creep at any distance relative to the punch radius is found to be proportional to the applied punching stress. As a result, the steady-state impressing velocity is proportional to the punch radius, and has the same stress dependence as the steady-state creep rate. The calculated impressing velocity agrees very well with the experimental value for the same conditions. For the power law constitutive equation,

$$\dot{\epsilon}_e = A\sigma_e^n, \tag{11}$$

where $\dot{\epsilon}_e$ is the unidirectional creep rate, σ_e is the unidirectional stress, and A and n are constants at constant temperature, the impressing velocity may be expressed by

$$v_d = 2Aa(\sigma/m)^n. \tag{12}$$

For the succinonitrile crystals used in this study at

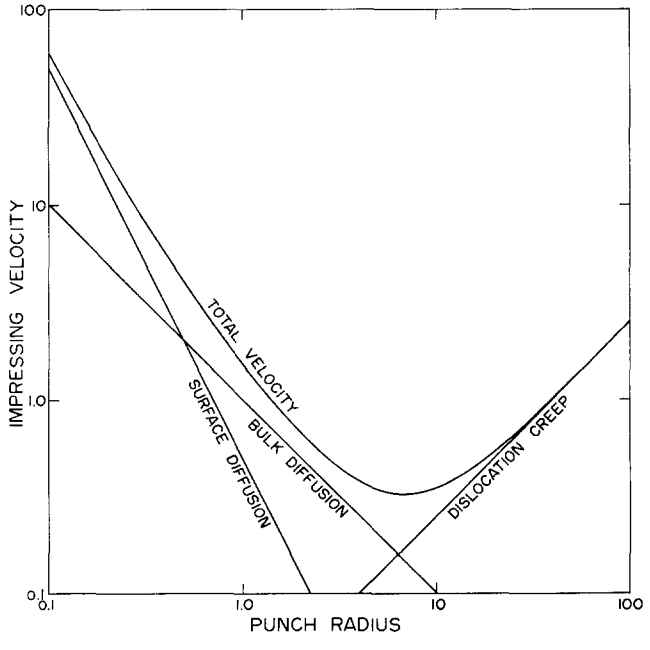

Figure 3 Effect of punch radius on impressing velocity for the three creep mechanisms.

37° C, A is found to be 0.84 and $n = 4$ when σ_e is in MN m^{-2} and $\dot{\epsilon}$ in sec^{-1}. For the same units, m is found to be 3.3 using experimental information to be presented later. This factor of 3.3 is comparable to the usual hardness/ strength ratios.

Since all three mechanisms can operate simultaneously in parallel [6], the overall impressing velocity is the sum of v_b, v_s, and v_d. The effects of punch size are shown in Fig. 3 where the regions of a^{-2}, a^{-1}, and a are separated for possible identification of the three mechanisms.

3. Material and creep apparatus

For experimental convenience, the b c c globular molecular crystal, succinonitrile, was used because of its low melting point, softness, and environmental stability. Reagent grade succinonitrile polycrystals were prepared under vacuum by the zone-melting method. Ingots of 1 in. diameter were grown. Samples of 1 in. diameter by 1.2 in. length were cut from the ingot. The cut surfaces were remelted and annealed around 10° C below melting point for more than 3 days until the surface became transparent. The grain size varied from 5 mm to less than 0.1 mm. The average grain size was about 1.2 mm.

The impression creep apparatus is shown schematically in Fig. 4. The sample is situated inside a brass cage, supported by a glass cylinder inside the furnace, in order to keep the temperature uniform throughout the entire sample. The temperature of the furnace is controlled to less than ±0.3° C. A cylindrical punch is attached to the lower end of the core of a linear displacement transducer (LVDT). The weight of the LVDT core is balanced by weights on the weight holder across a pulley. The load can be added either by reducing the balancing weight or by putting cylindrical weights with a central bore on top of the punch.

The impression distance is recorded continuously as a function of time. Limited by the low melting point of succinonitrile crystals which is about 58° C, data were taken at four different temperatures from 22° C to 44° C. Conventional creep testing was also performed under uniaxial compression to provide the power law constitutive equation in the finite element analysis.

4. Results and discussion

To illustrate first that the impressing velocity reaches a constant value, typical impressing depth–time curves are shown in Fig. 5 for several punching stresses. The slopes of these curves are plotted in Fig. 6 as a function of time. It is seen that the velocities clearly approach steady-state values for each punching stress. These steady-state velocities are plotted in Fig. 7 as a function of punching stress for five different punch diameters. It is seen that the power law of exponent 4.0 ± 0.1 holds for each punch size. The punch size-

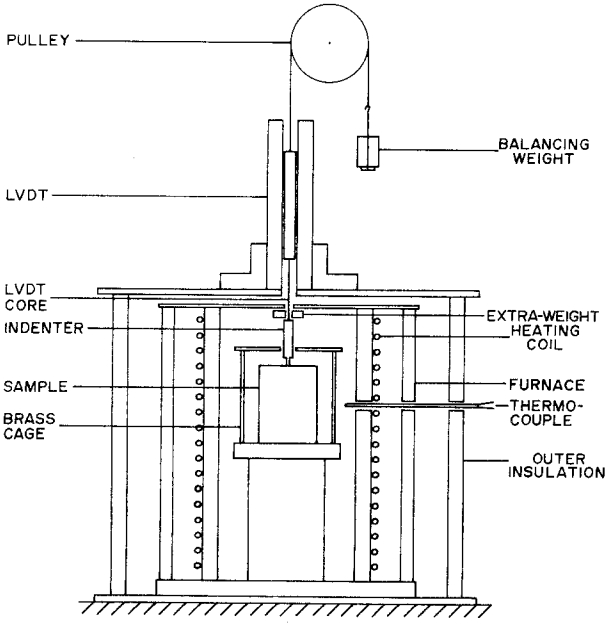

Figure 4 Apparatus for impression creep testing.

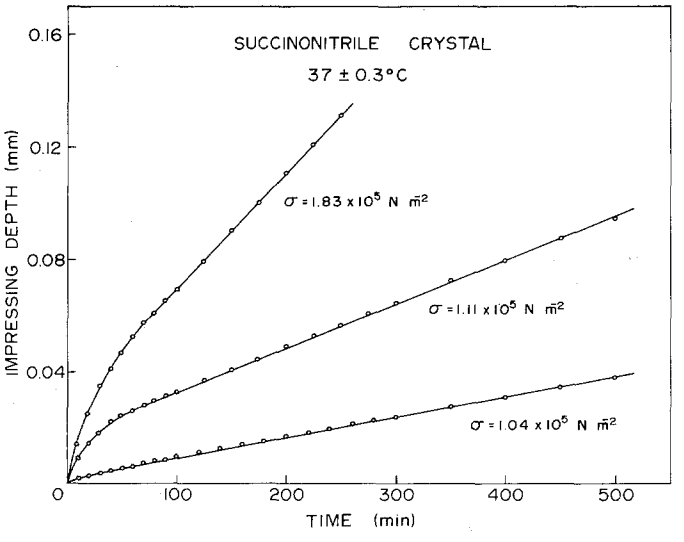

Figure 5 Impression creep curves for succinonitrile.

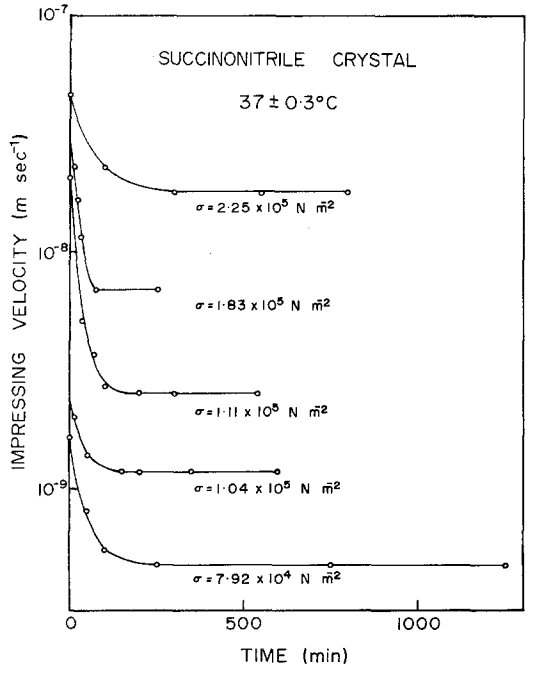

Figure 6 Time variation of impressing velocity.

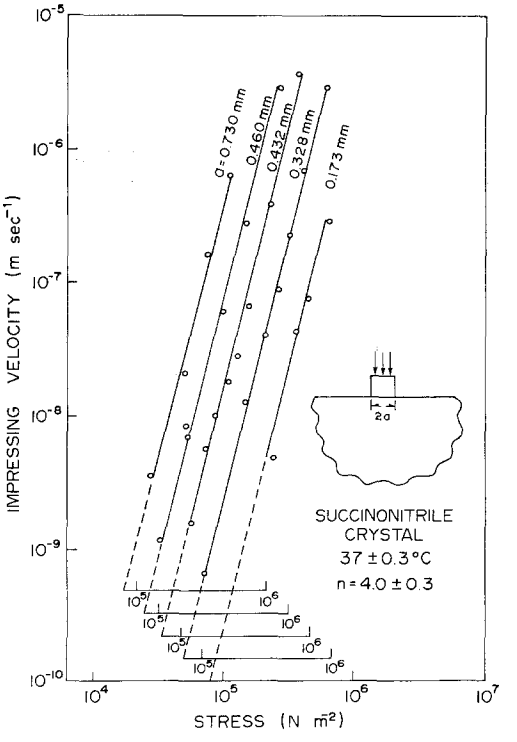

Figure 7 Stress dependence of impressing velocity.

dependence is shown in Fig. 8 at four stress levels revealing all linear relations. These results when compared with Fig. 3 and Equation 11 indicate that the impression creep is in the dislocation creep regime. The stress exponent is confirmed by performing conventional compression creep on samples of the same size at lower stresses to avoid bulging. The transient strain is about 1 to 2%. The results are shown in Fig. 9, confirming the stress exponent of 4. This stress exponent is comparable to a range of values of 4.1 to 5.4 reported by Hawthorne and Sherwood [7] from their conventional creep tests.

By using the self diffusivity as reported [7], it is possible to calculate the impressing velocity due to bulk diffusion from Equation 6. At 37° C, under a punching stress of 0.1 MN m^{-2}, and for a punch radius of 0.432 mm, v_b is calculated to be 4×10^{-13} m sec^{-1} which can be compared to about 10^{-9} m sec^{-1} in Fig. 7 for the same conditions.

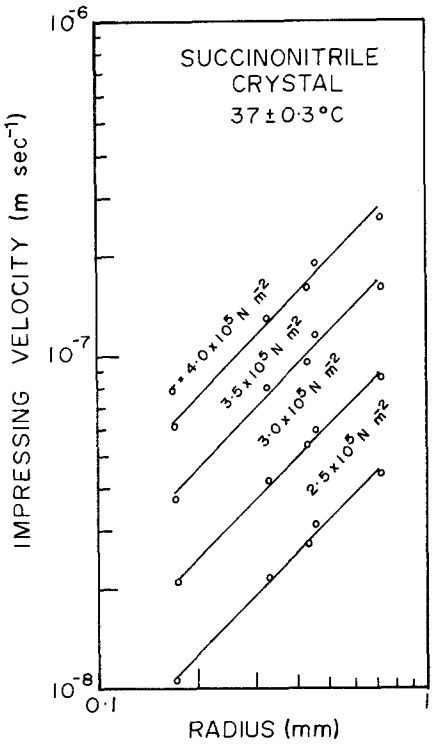

Figure 8 Effect of punch radius on impressing velocity.

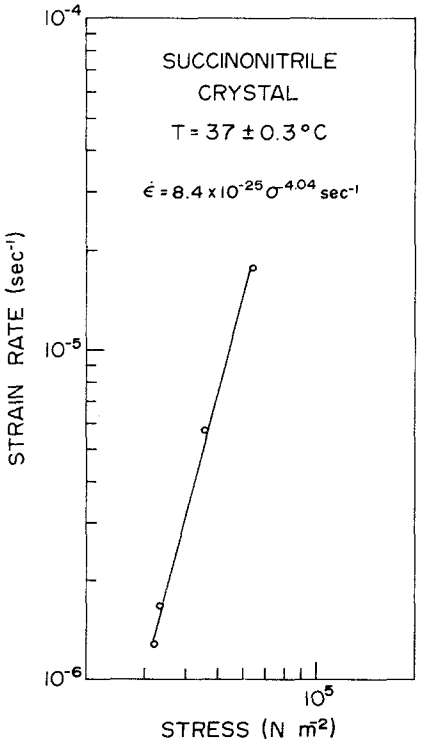

Figure 9 Stress dependence of conventional compression creep test.

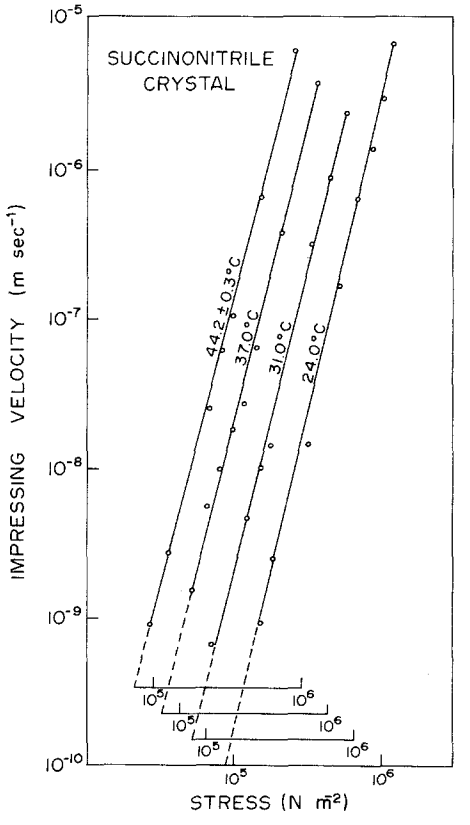

Figure 10 Temperature dependence of the power law relationship.

This comparison indicates that contributions from both bulk diffusion and surface diffusion to the impressing velocity are negligible under the present experimental conditions.

The effect of temperature is shown in Fig. 10. These data are replotted in Fig. 11 to obtain the activation energy as a function of punching stress, shown in Fig. 12. Also shown in Fig. 12 are the activation energies obtained from conventional creep tests reported by Hawthorne and Sherwood [7] on the same material. Although their stresses are much lower, the two sets of activation energies seem consistent with each other. The extrapolated value at zero stress, 14.2 kcal mol^{-1}, is comparable to the activation energy for self diffusion, 13.2 kcal mol^{-1} as reported in the literature [7].

As mentioned in the Introduction, two steady-state velocities are measurable when a cylindrical punch is pushed into the crystal at constant load: one near the surface and the other deep inside the specimen. An example is shown in Fig. 13. A transient stage and a steady-state stage are seen near the surface. When the punch descends further,

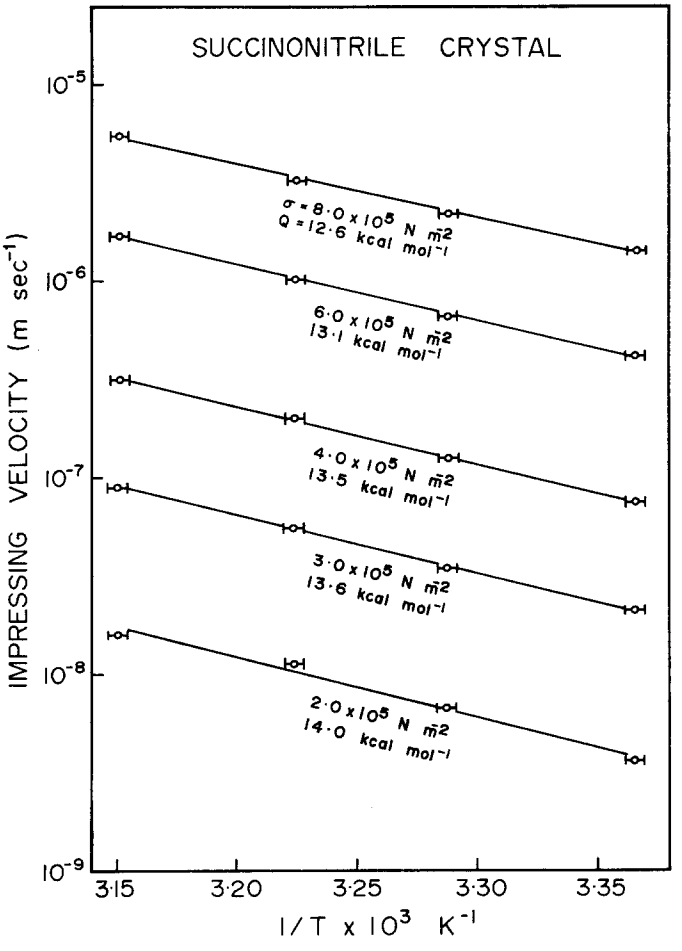

Figure 11 Temperature dependence of impressing velocity.

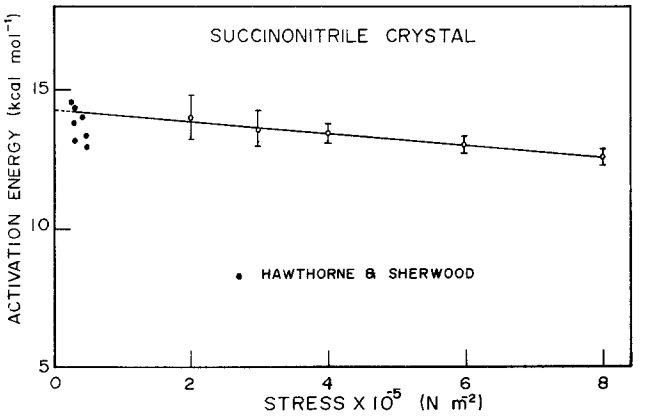

Figure 12 Activation energy for impression creep of succinonitrile.

this steady-state velocity gradually decreases to another steady state, deep inside the specimen. The velocities are plotted in Fig. 14 and it is seen that two stages of steady-state velocities are clearly definable.

Since the grain size of succinonitrile varies from 0.1 mm to 5 mm in the same crystal with an average value of 1.2 mm, and since the punch size is about the same (0.4 to 1.4 mm) as the grain size, the punch usually covers about a grain and the deformation is concentrated within it. The effect of grain-boundary sliding must be unimportant under the creep conditions reported, since otherwise the behaviour of small punches (smaller than grain size) should be quite different from that of large punches (larger than grain size). Indeed when the

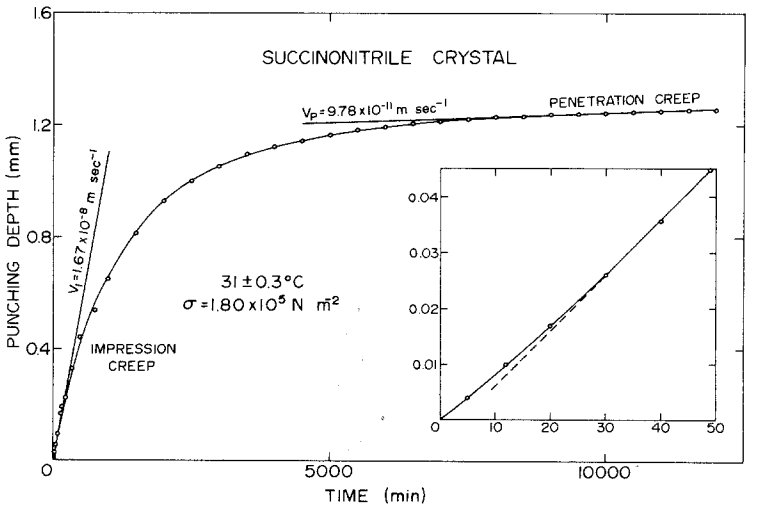

Figure 13 Impression creep and penetration creep, depth–time relations.

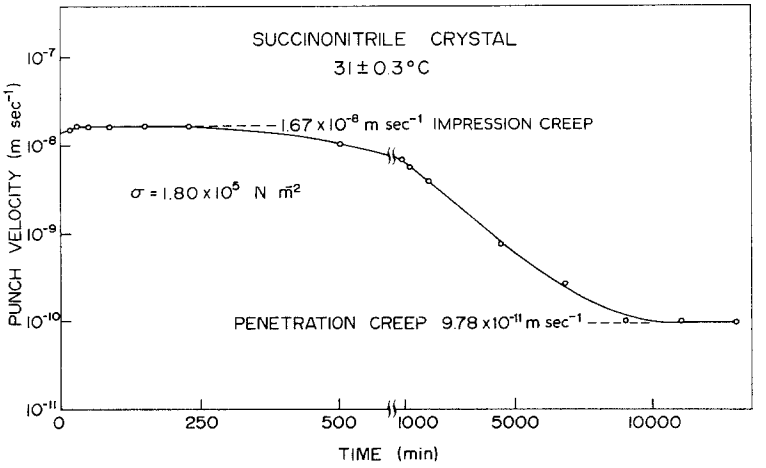

Figure 14 Impression creep and penetration creep, velocity–time relations.

punch size was about 2 mm, grain-boundary sliding was observed on the surface and the impressing velocity was abnormally high. These resutls are not included to avoid unnecessary confusion.

The foregoing results, together with the finite element analysis in the next paper, established the impression creep as a convenient way of obtaining creep information without using large quantities of material. Other advantages of impression creep are mentioned later.

5. Summary and Conclusions

(1) By using a cylindrical indenter, two steady state velocities are observed at constant load: one near the surface and the other deep inside the specimen. The former is called "impression creep" and the latter "penetration creep".

(2) Three mechanisms are possible for the impression creep of single crystals; bulk diffusion, surface diffusion and dislocation creep. In the diffusion regime, the impressing velocity is proportional to the punching stress while in the dislocation regime, a power law is observed. This power law has the same exponent as that in the conventional creep.

(3) For the same punching stress, the impressing velocity varies inversely with the punch diameter in the bulk diffusion regime, inversely with the punch area in the surface diffusion regime, and proportionally with the punch diameter in the dislocation regime. The latter is experimentally confirmed. These characteristics can be used to differentiate between mechanisms.

(4) The activation energy for impression creep

of succinonitrile crystals decreases slightly with increasing punching stress. The values are comparable to those in the literature from conventional creep studies.

(5) Some advantages of impressing creep testing are as follows: small amount of testing material, stress and temperature effects tested on the same crystal, stable deformation without tertiary stage, constant stress at constant load, separation of creep mechanisms by punch size effects in addition to stress and temperature effects, and possible direct determination of self diffusivities.

Acknowledgement

This work was supported by ERDA through contract EY-76-S-02-2296.*000.

References

1. J. H. WESTBROOK, *Trans. ASM* **45** (1953) 221.
2. H. D. MERCHANT, G. S. MURTY, S. N. BAHADUR, L. T. DWIVEDI and Y. MEHROTRA, *J. Mater. Sci.* **8** (1973) 437.
3. S. N. G. CHU and J. C. M. LI, TMS/AIME Fall Meeting, 1976, Niagara Falls, Abstract Bulletin, p. 61, E. C. Yu and J. C. M. Li, *ibid* p. 16.
4. S. N. G. CHU and J. C. M. LI, TMS/AIME Spring Meeting, 1975, Toronto, Abstract Bulletin p. 57.
5. J. C. M. LI, R. A. ORIANI, and L. S. DARKEN, *Z. physik. Chem. Neue Folge* **49** (1966) 271.
6. J. C. M. LI, in "Rate Processes in Plastic Deformation of Materials" edited by Li and Mukherjee (ASM, Columbus, Ohio, 1975) p. 479.
7. H. M. HAWTHORNE and J. N. SHERWOOD, *Trans. Faraday Soc.* **66** (1970) 1792.

Received 18 February and accepted 11 March 1977.